4. THERMAL SUBSIDENCE

A. THERMAL ISOSTASY

In an earlier section (Chapter 2, part C), we discussed an isostatic balance for a section of rifted lithosphere. It was noted that the long-term subsidence of the rift was associated with cooling and thickening of the lithosphere. Cooling causes the lithospheric rock to become more dense. To a first approximation, the density of the mantle lithosphere (ρ_L) varies with temperature (T) according to:

$$\rho_L = \rho_0 [1 - \alpha_V (T - T_0)] \qquad (4.1)$$

where: ρ_0 = density of lithospheric rock at 0 °C (3330. kg/m^3)
T_0 = surface temperature (0 °C)
α_V = volume coefficient of thermal expansion (3.28 x 10^{-5} K^{-1})

If the asthenosphere is nothing more than hot (T_1 = 1333 °C) mantle lithosphere, then we can calculate a density of 3184. kg/m^3 for the asthenosphere using equation 4.1. This suggests a density difference of only 4.4% between the coldest mantle lithosphere and the asthenosphere, but integrated over the entire thickness of the lithosphere temperature differences make a substantial contribution to the overall isostatic balance. In the following sections we will discuss a thermal model developed by McKenzie (1978) to describe the subsidence history of rift basins.

B. SIMPLE STRETCHING MODEL

McKenzie's (1978) simple stretching model was introduced in Chapter 2, part C. The initial subsidence (S_i) represents a tradeoff between crustal stretching, which causes subsidence, and thinning of the mantle lithosphere, which causes uplift. In our previous treatment of the initial subsidence problem, we assumed that stretching affects the thickness, but not the density, of the crust and mantle lithosphere. However, equation 4.1 suggests that heating of the lithosphere during rifting will reduce the density of the rifted lithosphere and affect the initial subsidence. In order to calculate the change in thermal structure of the

lithosphere during rifting, we need to know the prerift temperature distribution and how the lithosphere deforms during rifting. We assume that prior to rifting the temperature distribution of the lithosphere increases linearly from 0 °C at the surface to T_1 at the base of the lithosphere. If the stretching process is sufficiently rapid (we will quantify this in part H of this chapter) and homogeneous (constant strain rate) then the temperature distribution at the end of rifting will increase linearly from 0 °C at the surface to T_1 at the base of the thinned lithosphere. During rifting, the thermal gradient increases from T_1/a (where a is the lithosphere's thickness) to $\beta T_1/a$, because the lithosphere's thickness is reduced from a to a/β. Taking changes in both temperature and layer thickness into account (e.g., Fig. 4.1), it is straightforward to determine the initial or syn-rift subsidence:

$$S_i = \frac{a[(\rho_0-\rho_c)\,\frac{t_c}{a}\,(1-\frac{\alpha_V T_1 t_c}{2a})-\frac{\rho_0\,\alpha_V T_1}{2}](1-\frac{1}{\beta})}{\rho_0(1-\alpha_V T_1)-\rho_w} \qquad (4.2)$$

where t_c = initial thickness of crust (30-50 km)
ρ_c = density of continental crust (2800 kg/m^3)
ρ_w = density of water (1000 kg/m^3)

It is assumed that the surface of the crust was at sea level prior to rifting and that the subsided crust is covered by water. Initial subsidence will occur as long as the initial crustal thickness is greater than 17.2 km. If the crustal thickness is less then stretching will cause uplift. Figure 4.2 shows how the initial and total subsidence vary with the stretching factor (β) for an assumed crustal thickness of 35 km. The initial subsidence is simple to calculate because the temperature distributions before and after stretching are assumed (i.e., the dynamics of the rifting process are largely ignored). You will occasionally see the initial subsidence expressed in the form:

$$S_i = \frac{(\rho_0-\rho_c)}{(\rho_0-\rho_w)}\,t_c\,(1-\frac{1}{\delta})-\frac{\rho_0\,\alpha_V T_1}{2(\rho_0-\rho_w)}\,a\,(1-\frac{1}{\beta}) \qquad (4.3)$$

where the crust is assumed to have been stretched by δ and the mantle lithosphere by β. Also, in comparison to equation 4.2, some small terms have been dropped. For the case of uniform stretching, δ is equal to β. In equation 4.3, the first term represents subsidence due to crustal thinning, the second term represents uplift due to mantle lithosphere thinning. We will discuss nonuniform stretching models in part G of this chapter.

It is more difficult to determine the thermal subsidence that follows rifting, because the temperature structure and, consequently, the density structure of the lithosphere are *a priori* unknown. The thermal structure of the lithosphere can be calculated, however, using the initial temperature distribution (following stretching) and boundary conditions of $T = T_0$ at the surface and $T = T_1$ at the base of the lithosphere (Fig. 4.3). We also assume that secular cooling of the lithosphere is governed by one-dimensional thermal conduction. This means that we ignore heat transport via convection and lateral heat conduction. Using standard Fourier-series techniques (see section 3.4 of Carslaw and Jaeger, 1959) the temperature of the lithosphere, as a function of depth (z) and time since rifting (t), is given by:

$$\frac{T}{T_1} = \frac{z}{a} + \frac{2}{\pi} \sum_{n=1}^{\infty} \left[\frac{\beta}{n^2 \pi} \sin \left(\frac{n \pi}{\beta} \right) \right] \exp \left(- \frac{n^2 t}{\tau} \right) \sin \left(\frac{n \pi z}{a} \right) \qquad (4.4)$$

where: τ = thermal time constant $(a^2 / \pi^2 \kappa)$
κ = thermal diffusivity $(8 \times 10^{-7}\ m^2/s)$

Equation 4.4 is not as complicated as it looks. The first term on the right-hand-side is simply the long-term or steady-state temperature distribution shown in Figure 4.3. The summation represents the amount of excess temperature or heat brought into the lithosphere by the rifting process (Fig. 4.3). In fact, most of the excess heat is contained in the first term ($n = 1$) of the summation. As time passes, individual terms in the summation will become vanishingly small due to the exponential term involving time. This simply means that the excess heat is gradually removed by the process of conduction. The time constant (τ) controls the rate at which the lithosphere cools toward equilibrium. For the parameters that we have given, $\tau = 62.8$ My. Do not forget that time is

measured from the end of rifting. In using this equation to model lithospheric cooling, we ignore the thermal blanketing effect of the sedimentary cover. This effect is considered small as long as the sedimentary section is much thinner than the lithosphere (Turcotte and Ahern, 1977).

If we restrict our attention to the first term in the summation of equation 4.4, then the change in lithosphere temperature (ΔT) as a function of depth and time becomes:

$$\Delta T = -\frac{2\,T_1\,\beta}{\pi^2}\,sin(\,\frac{\pi}{\beta}\,)\,[\,1-exp(\,-\frac{t}{\tau}\,)\,]\,sin(\,\frac{\pi\,z}{a}\,) \qquad (4.5)$$

As noted earlier, we are justified in neglecting the higher order terms in the summation because most of the excess temperature is contained in this first term (n = 1). Using equation 4.1, we can see that this cooling causes an increase in the lithosphere density according to:

$$\Delta\rho_L = \frac{2\,\rho_0\,\alpha_V\,T_1\,\beta}{\pi^2}\,sin(\,\frac{\pi}{\beta}\,)\,[\,1-exp(\,-\frac{t}{\tau}\,)\,]\,sin(\,\frac{\pi\,z}{a}\,) \qquad (4.6)$$

Equation 4.6 represents the increase in density that occurs at any depth in the lithosphere at a given time after rifting has occurred. The greatest density increases are at mid lithosphere depths where temperature changes are largest. Notice that the thermal time constant (τ) controls the rate at which the lithosphere cools and becomes more dense. The final step is to relate the increase in density described by equation 4.6 to the thermal subsidence of the lithosphere. Figure 4.4 shows an isostatic balance between lithosphere that has just been stretched (t = 0) and partly equilibrated lithosphere (t > 0). The isostatic balance is given by:

$$S_T\,\rho_0\,[\,1-\alpha_V\,T_1\,] = \int_0^a \Delta\rho_L\,dz\; + S_T\,\rho_w \qquad (4.7)$$

where S_T is the amount of thermal subsidence that occurs following rifting. The term on the left represents the mass of asthenosphere

displaced as the lithosphere subsides, and the terms on the right represent the increase in lithospheric mass due to cooling and the mass of water that fills the basin. The basin is assumed to be filled to some datum (typically sea level) at all times. It is common practice to drop the term involving $\alpha_V T_1$ because of its small size, but note that this practice is inconsistent with the derivation of equation 4.2, which retains small terms. After making the appropriate substitutions and integrating equation 4.7, the thermal subsidence becomes:

$$S_T(t) = \frac{4 \rho_0 \alpha_V T_1 a}{\pi^2 (\rho_0 - \rho_w)} \left[\frac{\beta}{\pi} \sin\left(\frac{\pi}{\beta}\right) \right] \left[1 - exp\left(-\frac{t}{\tau}\right) \right] \qquad (4.8)$$

This approximate formula is valid as long as $\beta < 4$ but will work for $\beta > 4$ if $t > 20$ My (McKenzie, 1978). If your problem doesn't meet these conditions, you have to go back to the full summation in equation 4.3.

The total tectonic subsidence is just the sum of the initial and thermal subsidence:

$$S(t) = S_i + S_T(t) \qquad (4.9)$$

Figure 4.5 shows subsidence curves for crustal thicknesses of 30 and 40 km. Rifting is assumed to be instantaneous. It is clear that thermal subsidence is ultimately about the same magnitude as initial subsidence.

In the following sections we discuss how to fit the model to a given data set, and how to interpret the misfit between the model and data in terms of relative sea-level variations.

C. ESTIMATING THERMAL SUBSIDENCE PARAMETERS

We will assume that the basic parameters entering the thermal subsidence model (i.e., time of rifting, lithospheric thickness, and stretching factor) are unknown and then try to solve for these quantities by demanding that the theoretical model fit a tectonic subsidence data set in a least-squares sense. There is nothing sacred about least-squares curve-fitting techniques. In the real world, errors in the data seldom

follow a Gaussian distribution. If the technique yields parameter values that make no sense, ignore them.

To avoid carrying around a lot of parameters, let's rewrite equation 4.8 as:

$$S_T(t) = D_0\left[1 - exp\left(\frac{t - t_0}{\tau}\right)\right] \tag{4.10}$$

where

$$D_0 = \frac{4\,\rho_0\,\alpha_V T_1\,a}{\pi^2(\rho_0 - \rho_w)}\left[\frac{\beta}{\pi}\,sin\left(\frac{\pi}{\beta}\right)\right] \tag{4.11}$$

is the amount of thermal subsidence that will ultimately occur, t is now age (measured with respect to the present), and t_0 is the time (before present) when thermal subsidence began. We want to estimate the three model parameters D_0, t_0, and τ. Only rarely will you have a complete section (rift and postrift sediments) to analyze. For example, the COST B2 well, located on the Atlantic margin off New Jersey, penetrates only 4.8 km of an estimated 12.8-km-thick sedimentary sequence. We take a pragmatic approach to dealing with incomplete sections. Simply define a new datum (from which to measure tectonic subsidence) by setting the tectonic subsidence of the deepest stratum to zero (Fig. 4.6). The tectonic subsidence with respect to this new datum is:

$$w(t) = D_1\left[1 - exp\left(\frac{t - t_1}{\tau}\right)\right] \tag{4.12}$$

Although the time constant remains unchanged, we now have two new parameters D_1 and t_1. D_1 is the ultimate amount of tectonic subsidence that will occur with respect to the new datum, and t_1 is the time (before present) when the thermal subsidence curve passes through the datum. Comparing equations 4.10 and 4.12, you can see that the relationship between the four parameters D_0, t_0, D_1, and t_1 is:

$$D_0 = D_1\,exp\left(\frac{t_0 - t_1}{\tau}\right) \tag{4.13}$$

There is a bit of a snag here. By fitting the thermal subsidence model to a given data set we will obtain estimates for D_1, t_1, and τ. But equation 4.13 shows that it will be impossible to obtain independent estimates of D_0 and t_0. Obviously, we will need some supplementary information about D_0 or t_0 in order to complete the analysis. For now, we continue with our attempt to estimate the model parameters in equation 4.12.

Tectonic subsidence data typically consists of N triplets of numbers (t_i, $w_{min,i}$, $w_{max,i}$) where i = 1, 2, 3, ..., N. The first quantity (t_i) is an age, and the last two quantities ($w_{min,i}$, $w_{max,i}$) are the minimum and maximum estimates of tectonic subsidence at that age. We use the average of the maximum and minimum subsidence estimates to estimate the model parameters:

$$w_i = \frac{1}{2}\left(w_{i,\,max} + w_{i,\,min}\right) \tag{4.14}$$

and one-half of the difference between the subsidence estimates to estimate the uncertainty in the data:

$$\sigma_i = \frac{1}{2}\left(w_{i,\,max} - w_{i,\,min}\right) \tag{4.15}$$

Because we are solving for three unknown quantities, we need at least three triplets of data ($N \geq 3$). Be sure that the data come from the postrift portion of the subsidence history; that is where the thermal subsidence model applies. We assume that optimal parameter values are those that minimize the sum of the squares of the misfit between the theoretical subsidence (from equation 4.12) and the data:

$$\chi^2(D_1, t_1, \tau) = \sum_{i=1}^{N} \left\{ \frac{w_i - D_1\left[1 - exp\left(\frac{t_i - t_1}{\tau}\right)\right]}{\sigma_i} \right\}^2 \tag{4.16}$$

We solve for the model parameters using a version of the Levenberg-Marquardt algorithm for nonlinear least-squares problems developed by Press et al. (1986). Be aware that nonlinear least-squares algorithms tend to get trapped in local minima of the function χ^2, thereby

missing the true minimum. Initial guesses for the parameters should be varied to ensure that the algorithm has found the true minimum.

You should realize that the whole point of the least-squares technique is to minimize the misfit between a physical model and the data set. Because we will be interpreting deviations from the theoretical model in terms of relative sea-level variations, the least-squares technique will tend to minimize sea-level variations. To avoid underestimating sea-level variations, it is important to include any geological or geophysical constraints that exist for the stretching factor and time of onset of thermal subsidence.

D. EXAMPLE I–SUBSIDENCE EXAMPLE

In the previous chapter we calculated a tectonic subsidence history by making corrections for compaction, Airy compensation, and water depth variations. Let's use that data set to constrain the thermal subsidence model using the technique from the previous section. Our data is listed in Table 4.1, and plotted in Figure 4.7.

From the least-squares algorithm, we determined the following set of parameters with $\chi^2 = 3.8$ km^2:

$$D_1 = 2.2 \pm 0.1\ km \tag{4.17a}$$

$$t_1 = 95.9 \pm 21.2\ Ma \tag{4.17b}$$

$$\tau = 23.6 \pm 14.9\ My \tag{4.17c}$$

Our estimates of parameter uncertainty are obtained by interpreting the diagonal elements of the covariance matrix (a byproduct of the curve-fitting algorithm) as the squares of the standard deviations of the parameters. There is considerable uncertainty in the thermal time constant, but this is not surprising given the large uncertainties in paleowater depths. The resulting thermal subsidence curve (from equation 4.12) is shown in Figure 4.7.

Let's return now to the problem of calculating D_0 and t_0. For this example, we are fortunate to know that thermal subsidence begins at 70 Ma. Letting t_0 = 70 Ma in equation 4.13, we can solve for D_0:

$$D_0 = 0.7\ km \tag{4.18}$$

Knowing τ, we can calculate the lithosphere's thickness:

$$a = \pi\sqrt{\kappa\tau} = 76.7 \pm 24.2\ km \tag{4.19}$$

and the stretching factor (using the thermal subsidence term in equation 4.2 with D_0):

$$\beta = \left\{1 - \frac{2 D_0 \left[\rho_0(1 - \alpha_V T_1) - \rho_w\right]}{\alpha_V a T_1 \rho_0}\right\}^{-1} = 1.4 \tag{4.20}$$

We can also use equation 4.11 to calculate β, but this is more difficult because D_0 is not a simple function of β:

$$\frac{\beta}{\pi} sin\left(\frac{\pi}{\beta}\right) = \frac{\pi^2 D_0 \left[\rho_0(1 - \alpha_V T_1) - \rho_w\right]}{4\ \alpha_V a T_1 \rho_0} \Rightarrow \beta = 1.4 \tag{4.21}$$

Equations 4.20 and 4.21 may not always yield the same value for β, because equation 4.7 (from which equation 4.21 was derived) is only the first term of an infinite series.

At this stage, we could use the initial tectonic subsidence, calculated in Chapter 2, to calculate a crustal stretching factor. To do so, we would need to measure the prerift crustal thickness (t_c). Instead, we turn to an interpretation of the misfit between the subsidence data and the theoretical subsidence model.

E. RELATIVE SEA-LEVEL VARIATIONS

Figure 4.8 shows minimum and maximum estimates of water-depth variation (with respect to the present) using the data and best-fitting thermal model from the previous section. We made this plot by

subtracting the calculated (maximum and minimum) values of tectonic subsidence from the theoretical amount of thermal subsidence. We then shifted each data set vertically so that the present-day water-depth variation is zero. Positive water depths indicate deeper water than at present. There are at least three ways to explain the observed variation: eustatic sea-level variations, fluctuations in sedimentation rates, and variations in rate of tectonic subsidence. Nobody knows how to isolate one of these factors and discern its history from the water-depth variations. Let's simply assume that water-depth variations are caused by eustatic sea-level changes, and proceed with our calculations.

In Chapter 3, we noted that an increase in water depth (ΔW_d) is related to an increase in eustatic sea-level (ΔSL) by:

$$\Delta SL = \left[\frac{\rho_m - \rho_w}{\rho_m}\right] \Delta W_d \qquad (4.22)$$

where the density ratio accounts for isostatic subsidence due to an increase in sea level. The density ratio's value is approximately 0.7. Using equation 4.22, we can convert the water-depth variation to a eustatic sea-level history (Fig. 4.9). Please don't compare this history with the Vail curves; we manufactured our data set. Also, keep in mind our caveat about separating the influences of sedimentation and tectonics from eustatics. It's more accurate to say that Figure 4.9 shows relative (as opposed to eustatic) sea-level variations. Watts and Steckler (1979) discuss how to isolate a eustatic history by analyzing the subsidence history of a number of wells.

F. EXAMPLE II--ANALYSIS OF SUBSIDENCE AT THE COST B2 WELL

Speculation on the petroleum potential of the continental margin of the eastern United States led to the drilling of a number of deep test wells during the late 1970s. The COST B2 well was drilled in the Baltimore Canyon Trough, southeast of New Jersey (Scholle, 1977). As was mentioned earlier, the COST B2 well penetrates 4.8 km of an estimated 12.8-km-thick sedimentary sequence. Steckler and Watts (1978) backstripped sediments from that well to obtain a tectonic subsidence history. Watts and Steckler (1979) estimate that the time

constant τ is in the range of 52 to 60 My, implying a lithosphere thickness of 113 to 121 km. Our analysis will show a considerably larger time constant and thicker lithosphere. We think the discrepancy exists because Watts and Steckler (1979) mixed syn- and postrift subsidence data together when estimating their thermal subsidence parameters. Also, they linearized the subsidence equation before fitting it to the subsidence data.

We use the basal strata of the COST B2 well as a datum, and tectonic subsidence data from Steckler and Watts (1978; their table 1). In Table 4.2 we list the subsidence data that were corrected for local isostatic compensation; the data is plotted in Figure 4.10.

We were unable to obtain a reasonable set of parameters using the definition of σ_i given in equation 4.15, so we arbitrarily assumed that σ_i = 1.0 m. The least-squares algorithm yields the following parameters for χ^2 = 0.137 km^2:

$$D_1 = 1.86\ km \tag{4.23a}$$

$$t_1 = 146.8\ Ma \tag{4.23b}$$

$$\tau = 97.8\ My \tag{4.23c}$$

The lithosphere's thickness is:

$$a = \pi\sqrt{\kappa\tau} = 156.\ km \tag{4.24}$$

The best-fitting thermal subsidence curve is shown with the data in Figure 4.10. The exact time at which thermal subsidence began is uncertain, but it probably is in the range of t_0 = 195 to 175 Ma. For t_0 = 195 Ma, we find:

$$D_0 = D_1 \exp\left(\frac{t_0 - t_1}{\tau}\right) = 3.0\ km \tag{4.25}$$

and a stretching factor of:

$$\beta = \left\{ 1 - \frac{2 D_0 \left[\rho_0 (1 - \alpha_V T_1) - \rho_w \right]}{\alpha a T_1 \rho_0} \right\}^{-1} = 2.4 \qquad (4.26)$$

For t_0 = 175 Ma, we obtain:

$$D_0 = D_1 \exp \left(\frac{t_0 - t_1}{\tau} \right) = 2.5 \; km \qquad (4.27)$$

and a stretching factor of:

$$\beta = \left\{ 1 - \frac{2 D_0 \left[\rho_0 (1 - \alpha_V T_1) - \rho_w \right]}{\alpha a T_1 \rho_0} \right\}^{-1} = 1.9 \qquad (4.28)$$

The upper bound on D_0 suggests that 2.6 km of thermal subsidence has occurred near the well whereas the lower bound suggests only 2.1 km. Steckler and Watts (1978) calculate that a total of 5.2 km of tectonic subsidence has occurred in the well's vicinity. This suggests initial subsidence of 3.1 to 2.6 km. One way to check our estimates of β and D_0 is to calculate crustal thickness using equation 4.3 (with $\delta = \beta$) and the estimates of initial subsidence:

$$t_c = \frac{(\rho_0 - \rho_w)}{(\rho_0 - \rho_c)} \frac{\beta S_i}{(\beta - 1)} + \frac{\alpha T_1 a \rho_0}{2 (\rho_0 - \rho_c)} = 41 \; to \; 50 \; km \qquad (4.29)$$

The smaller crustal thickness corresponds to t_0 = 195 Ma, the larger to t_0 = 175 Ma. Seismic refraction studies suggest that the normal crustal thickness along the U.S. Atlantic margin is 35 to 40 km. Perhaps we have underestimated D_0 by assuming the lithosphere is always locally compensated. A further complication to modelling initial subsidence is the average density of the crust may be substantially increased during the rifting process as a result of magmatism.

This finishes our analysis of the subsidence data. We turn next to a discussion of several twists that have been added to the simple stretching model in order to accommodate data from the real world.

G. NONUNIFORM STRETCHING MODELS

Royden and Keen (1980) tried to apply the simple stretching model to well data from the Nova Scotia and Labrador shelves. They found that the initial subsidence on these margins is considerably overestimated by equation 4.2 (see Fig. 4.11). Remember that initial subsidence is controlled by the interplay between crustal thinning (which promotes subsidence) and thinning of the mantle lithosphere (which promotes uplift). To reduce initial subsidence the mantle lithosphere must be thinned more than the crust. This can be accomplished by thickening the rifted crust by volcanic additions or by actually stretching the mantle lithosphere more than the crust.

Royden and Keen (1980) took the second approach (Fig. 4.12), stretching the crust by a factor of δ and the mantle lithosphere by a factor of β (see equation 4.3). Uniform stretching occurs when $\delta = \beta$. The initial subsidence is shown graphically in Figure 4.13 for a crustal thickness of 35 km and lithosphere thickness of 125 km. Initial uplift can occur when the mantle lithosphere is stretched by a large amount compared to the amount the crust is stretched. Thermal subsidence will not be significantly affected by differential stretching, unless there is a great disparity in the stretching factors. The ultimate amount of tectonic subsidence is still controlled by the amount of crustal thinning. Figure 4.11 shows theoretical subsidence histories applied to well data on the Labrador margin.

Nonuniform stretching is not well understood. Some workers argue that mantle lithosphere and crust are stretched by equal amounts on a regional basis. If this is true, local differences in stretching may be attributed to ductility contrasts between crust and mantle rocks. An elegant regional study of rifting in the Gulf of Suez (Steckler, 1985) suggests that the mantle lithosphere has been extended by 60 to 110 km, whereas crustal extension amounts to only 25 to 30 km. Steckler attributed the differential extension to lateral heat conduction and small-scale convection of heated mantle lithosphere. It is not that the mantle lithosphere has been extended more than the crust, but rather that the mantle lithosphere has been thinned by various heat transfer processes.

H. FINITE RATES OF EXTENSION

During rifting, at least two heat transport processes are active. The first is thermal convection; stretching physically carries hot rock up from depth toward the surface. Convection causes isotherms to bunch up and raises the surface heat flux. The time scale for this process is the duration of rifting (5 to 30 My, perhaps). The second process is thermal diffusion, which we have already considered. As isotherms get bunched up (due to convection) excess heat is diffused down the geothermal gradient to the surface. Diffusion tries to prevent the isotherms from getting bunched up.

As we have seen, the time scale for thermal diffusion is the thermal time constant τ (~60 My). Because of the difference in the time scales of these two processes, convection commonly wins out, and the lithosphere is heated and thinned during rifting. It is, however, important to remember that there are two possible end members to the rifting process. The first end member is instantaneous rifting where convection dominates. This is just McKenzie's simple stretching model in which subsidence is divided into two phases, initial followed by thermal. The other end member is infinitely slow (compared to τ) rifting where diffusion dominates. In this case, the lithosphere will remain in thermal equilibrium as stretching proceeds. At the end of rifting no thermal subsidence will occur. All subsidence occurs during the rifting phase. These two end members are shown schematically in Figure 4.14 where t = 0 marks the end of rifting. Real subsidence data should fall somewhere between these extremes. In this section we look at a model by Jarvis and McKenzie (1980) that offers some guidelines on applying the simple stretching model to the real world.

Jarvis and McKenzie (1980) considered a section of lithosphere undergoing uniform extension at some strain rate G. It is straightforward to show that the stretching factor will vary with the duration of rifting (t) according to:

$$\beta = exp(Gt) \tag{4.30}$$

To get some feeling for the magnitudes involved, note that if $\beta = 4$ and extension occurs at the uniform rate of $G = 10\%/My = 0.1\ My^{-1}$, then rifting has lasted:

$$t = log(\beta) / G = 14.\ My \tag{4.31}$$

In combined advection-diffusion problems, a nondimensional parameter called the Peclet number shows up. Loosely speaking, the Peclet number gauges the relative influence of advection and diffusion on heat transport. Large Peclet numbers indicate that advection dominates, whereas small values indicate that diffusion dominates. The appropriate Peclet number for the finite rate-of-rifting problem is:

$$G' = \frac{G\,a^2}{\kappa} \tag{4.32}$$

Figure 4.15 (from Jarvis and McKenzie, 1980) shows the temperature distribution in the lithosphere for a range of Peclet numbers, assuming $\beta = 4$ and $a = 125$ km. The instantaneous rifting model corresponds to an infinite Peclet number (i.e., an infinitely high strain rate). When $G' = 0$, the strain rate is zero, and the lithosphere remains in thermal equilibrium during rifting. It is clear that for $G' > 50$, the initial geotherm is close to that assumed in the instantaneous rifting model.

From their numerical calculations, Jarvis and Mckenzie (1980) developed a rule of thumb for deciding whether or not the instantaneous rifting model is a reasonable assumption for modeling subsidence. The duration of rifting (t) should obey the conditions:

$$t < \frac{60}{\beta^2} \qquad for\ \beta \le 2 \tag{4.33a}$$

$$t < 60\left(1 - \frac{1}{\beta}\right)^2 \quad for\ \beta \ge 2 \tag{4.33b}$$

If $\beta = 4$, then the duration of rifting must be less than 34 My, whereas if $\beta = 2$, the duration of rifting should be less than 15 My. If your basin doesn't meet these conditions, you should not try to analyze its subsidence using

the simple stretching model. You will need to use the full advection-diffusion model outlined in Jarvis and McKenzie (1980) or Cochran (1983).

I. LATERAL HEAT CONDUCTION

Another drawback of the simple stretching model is that it allows for one-dimensional (vertical) heat conduction only. If you consider that unstretched lithosphere adjacent to a rift basin will be cold, then it is clear that heat from the rift is likely to be conducted laterally as well as vertically. The effect of lateral heat conduction on subsidence is easy to understand. Lateral heat flow simply allows the rifted lithosphere to cool faster than it would by vertical conduction alone and implies that the lithosphere should subside more rapidly (at least during the early stage of thermal subsidence) than predicted by the simple stretching model (Fig. 4.16).

Lateral heat conduction should be most important close to the basin margin and less important far away. As a rule of thumb, lateral heat conduction can be safely ignored if you are considering the subsidence of a rift basin that is wider than the equilibrium thickness of the lithosphere (e.g., ~125 km). It is clear that lateral heat conduction will not affect the total subsidence, which depends only on the amount of crustal thinning. Unstretched lithosphere adjacent to rifts may be uplifted for a few tens of millions of years due to heating.

Figure 4.17 (from Sawyer et al., 1987) shows the predicted tectonic subsidence for the Los Angeles Basin, which was treated as a narrow rift basin. Heat was allowed to escape from the rift in two directions, one vertical and the other horizontal. Over the course of 11 My, tectonic subsidence is 1 km greater than the prediction of the simple stretching model. This is an extreme case because the maximum width of the rift is only 30 km.

Table 4.1
Example Data

Age, Ma	Minimum Depth, km	Maximum Depth, km
70	1.29	1.82
60	1.48	1.86
50	1.82	1.91
30	2.23	2.71
20	1.92	2.71
10	1.92	2.42
0	2.00	2.20

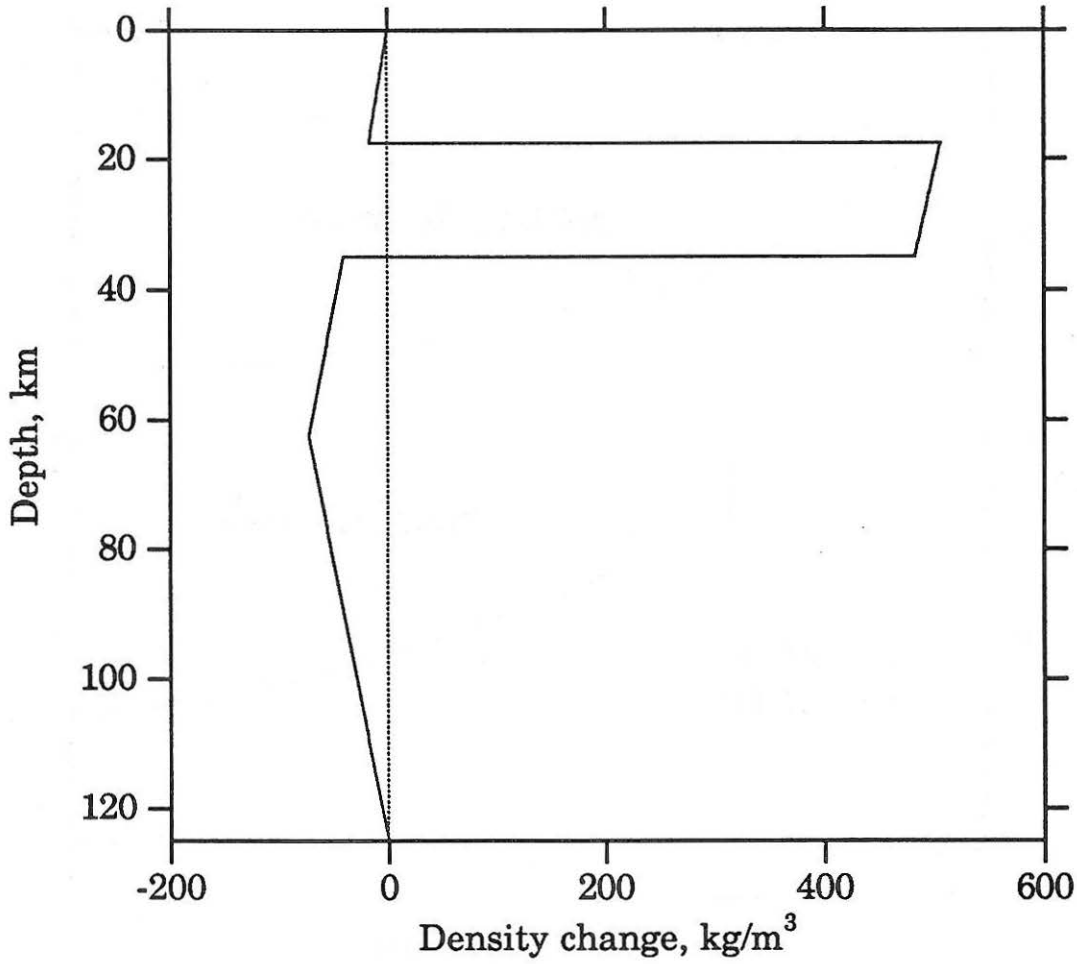

Figure 4.1 Density changes occur when lithosphere is stretched by $\beta = 2$. Original thickness of crust and lithosphere is 35 km and 125 km, respectively. Shallow zone of increased density is due to mantle lithosphere replacing crust. Zones of decreased density are due to heating of the crust and mantle lithosphere, and replacement of mantle lithosphere by asthenosphere.

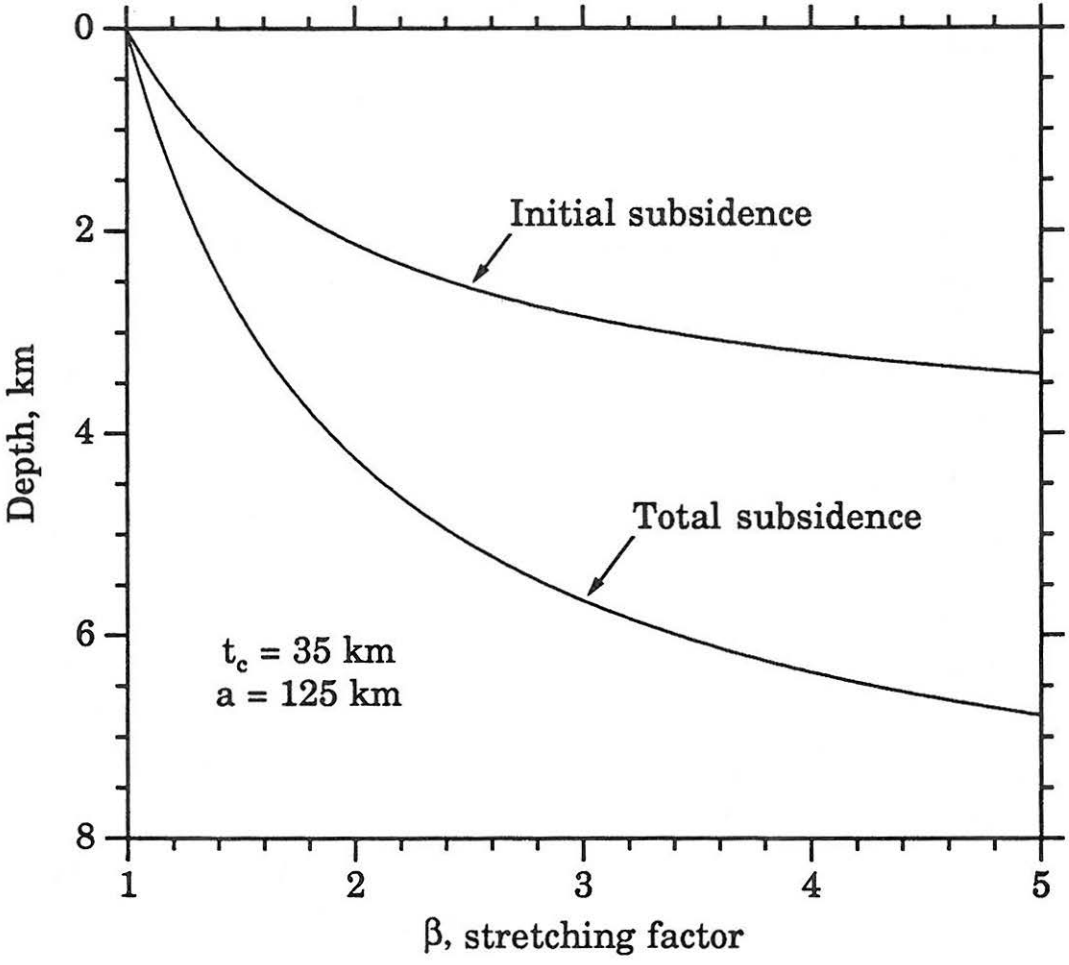

Figure 4.2 Initial and total subsidence as a function of the stretching factor β. Thickness of crust and lithosphere is 35 and 125 km respectively.

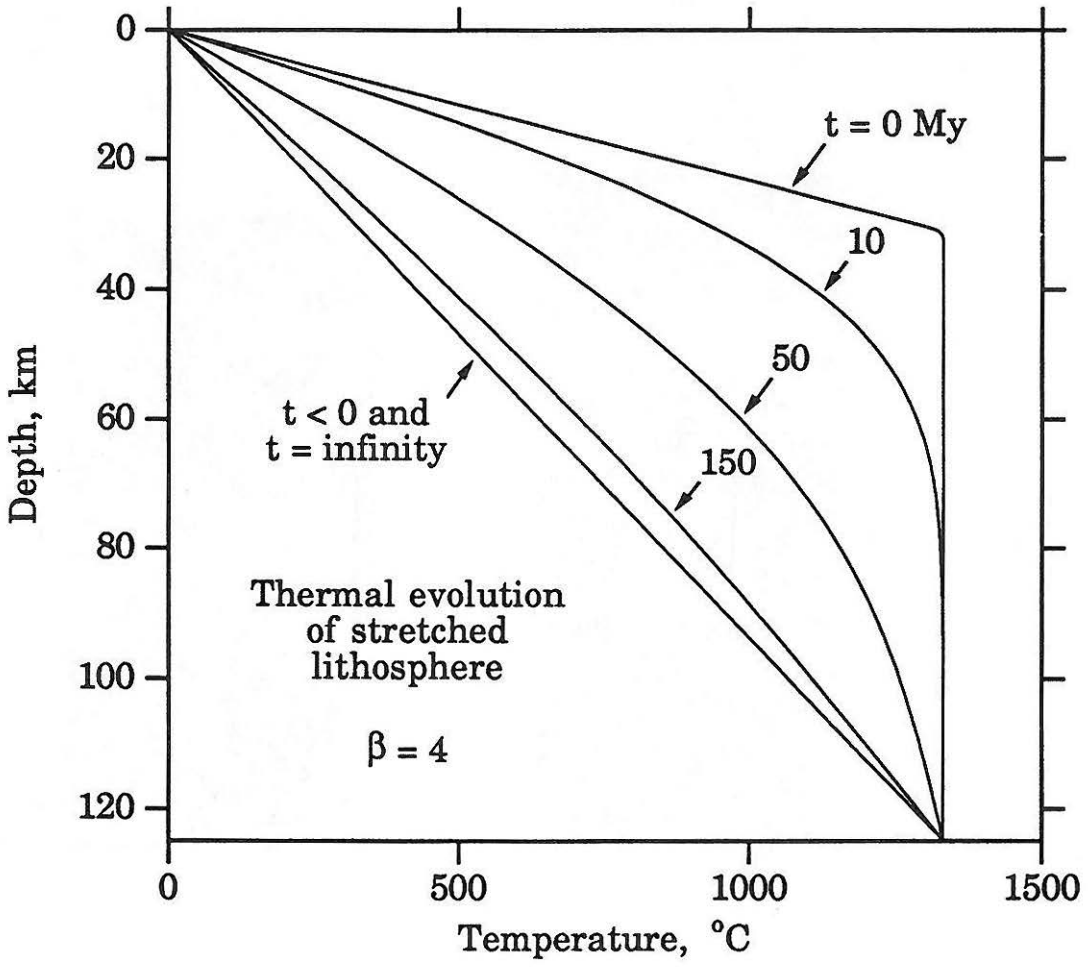

Figure 4.3 Cooling of the lithosphere following rifting (from equation 4.4). Thickness of lithosphere is 125 km and $\beta = 4$.

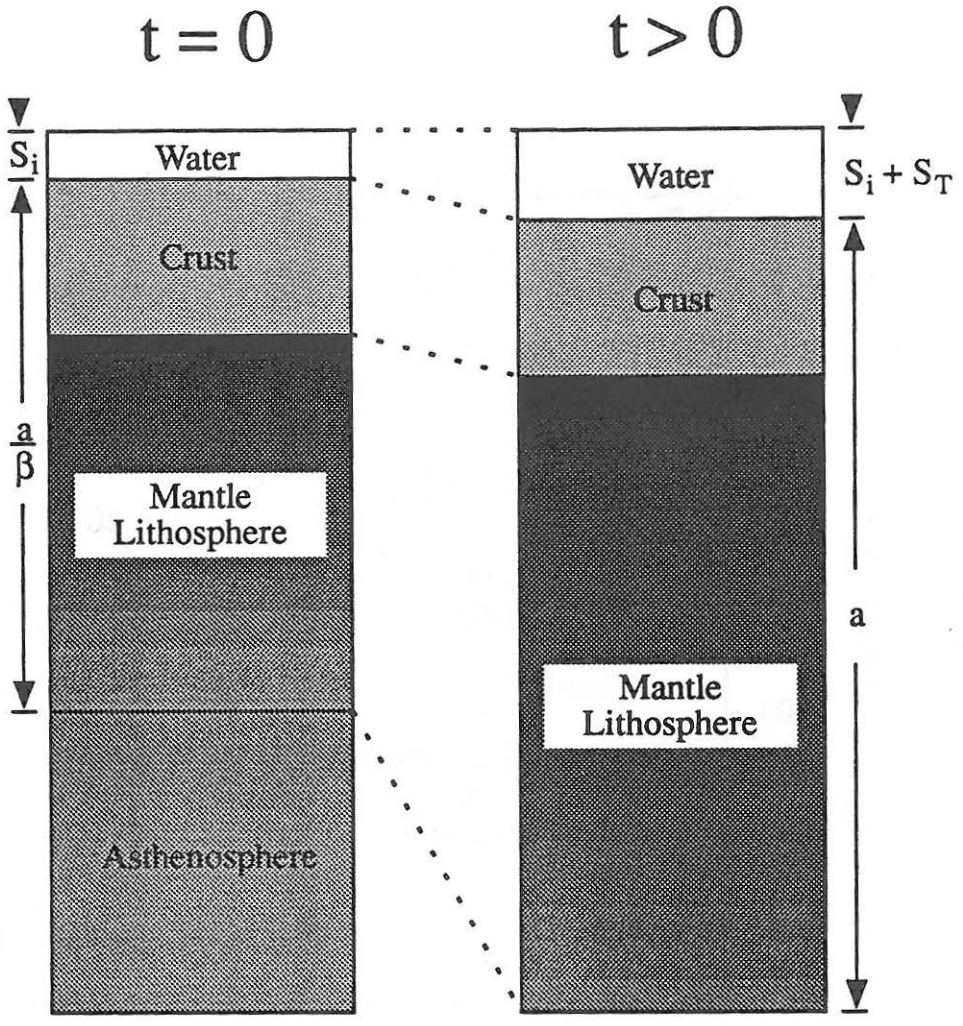

Figure 4.4 Isostatic balance between newly stretched lithosphere (at left) and partially re-equilibrated lithosphere (at right). Initial depths of various interfaces are given. S_i is the initial subsidence that accompanies stretching, S_T is the amount of thermal subsidence that occurs after rifting is finished.

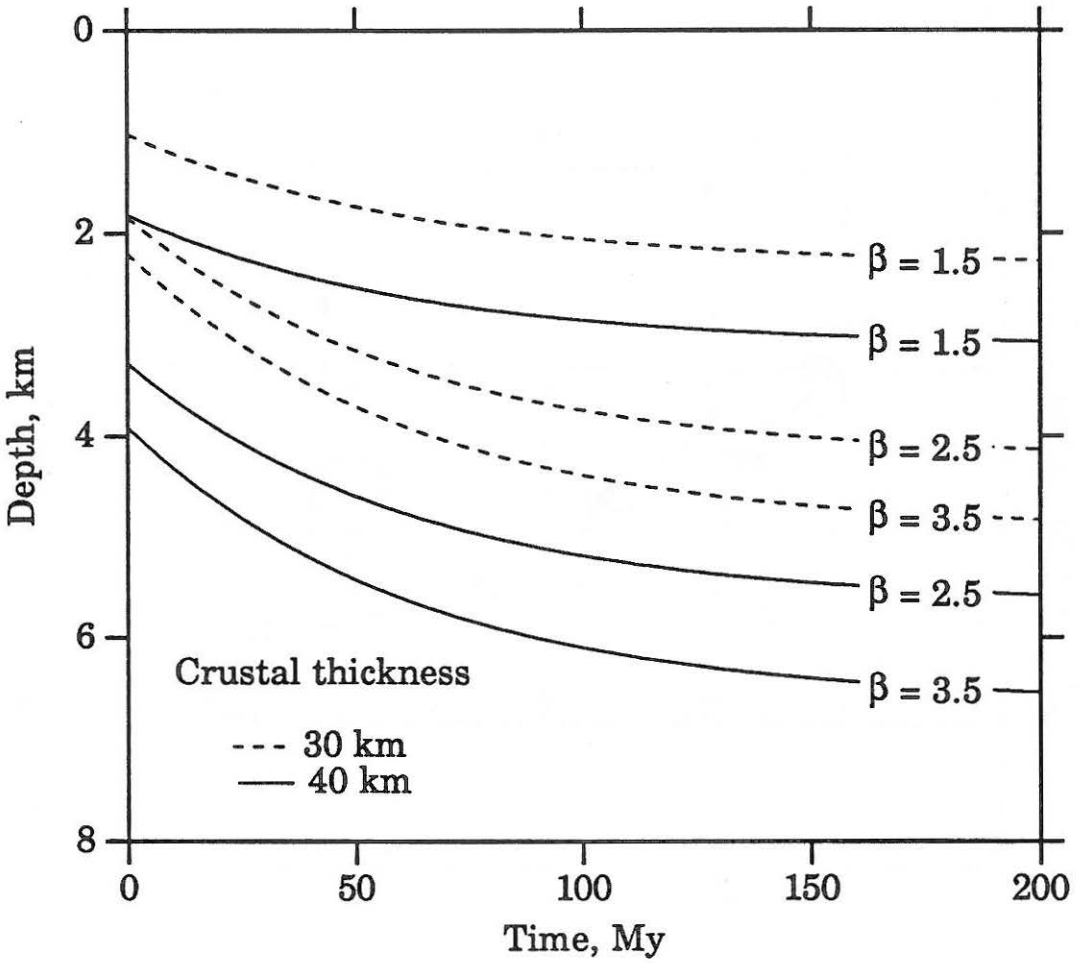

Figure 4.5 Initial and thermal subsidence histories predicted by Mckenzie's (1978) simple stretching model. Crustal thicknesses of 30 and 35 km are used. Lithosphere's thickness is 125 km.

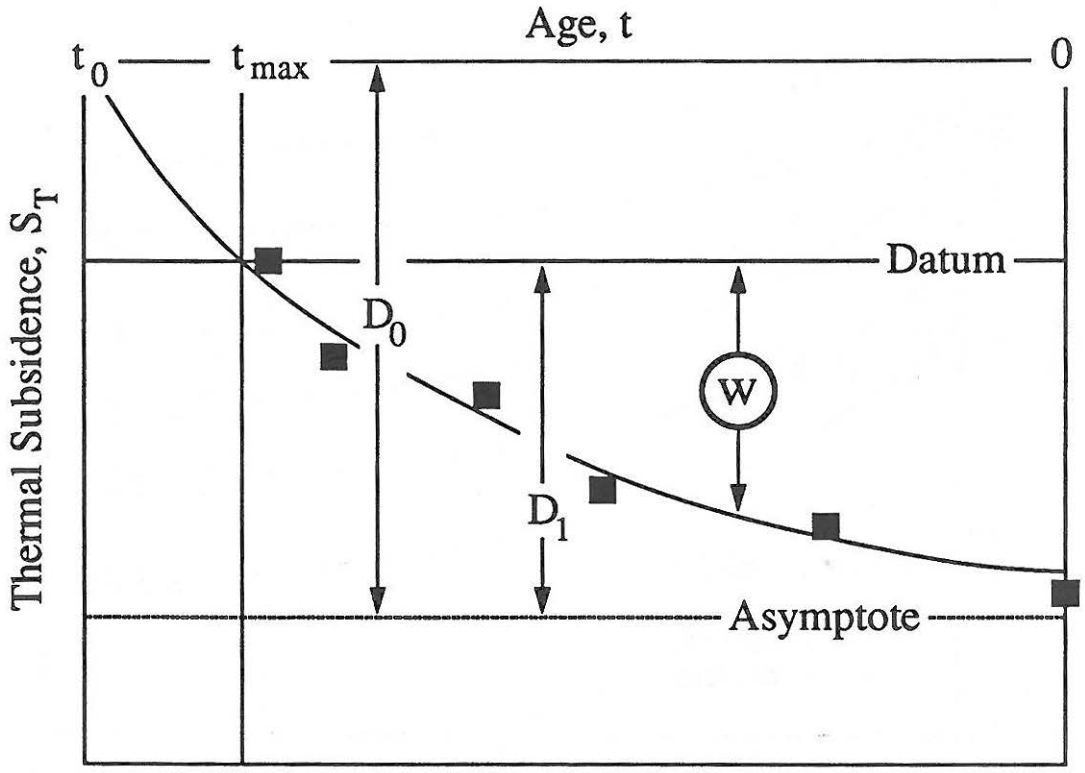

Figure 4.6 Reference frame used to analyze thermal subsidence in an incomplete sedimentary sequence. See text for explanation.

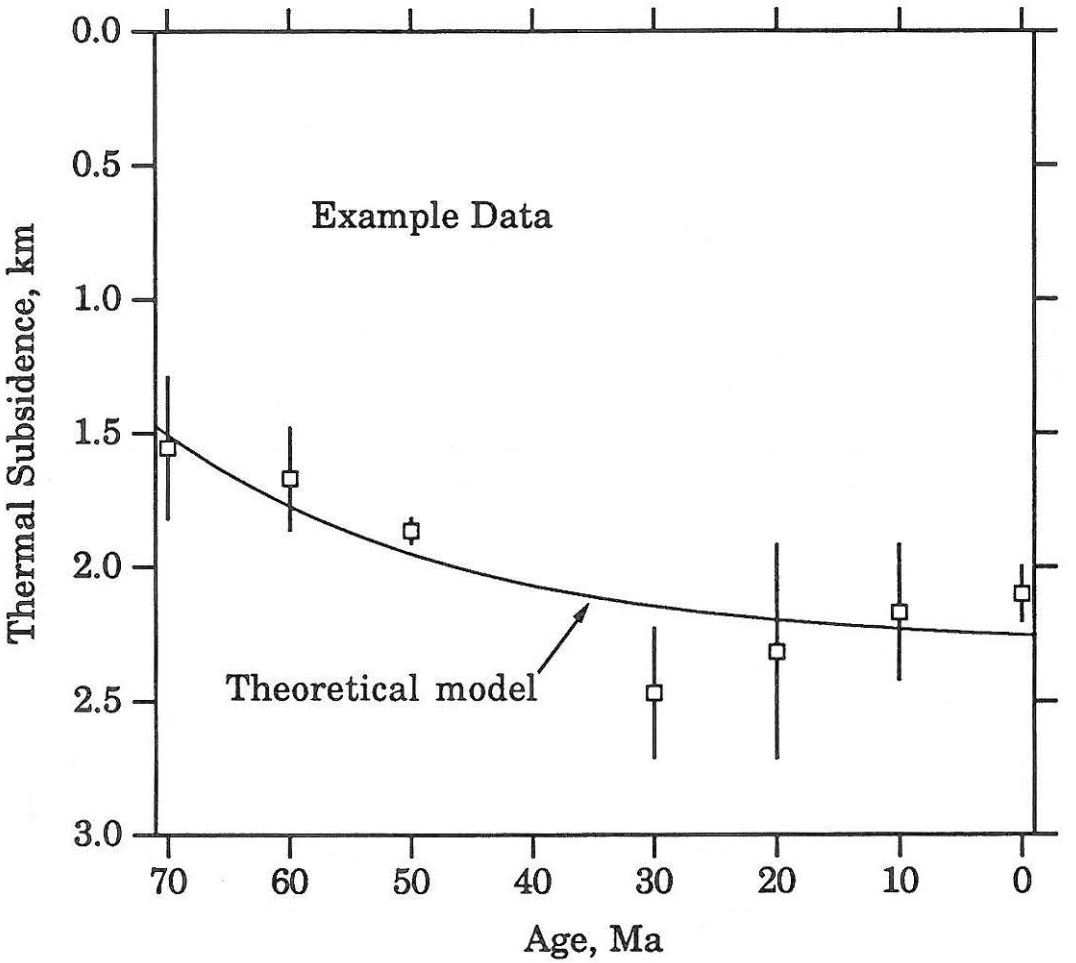

Figure 4.7 Tectonic subsidence data from example discussed in Chapter 3. Also shown is thermal subsidence history predicted by Mckenzie's simple stretching model. Model parameters were estimated using the least-squares technique.

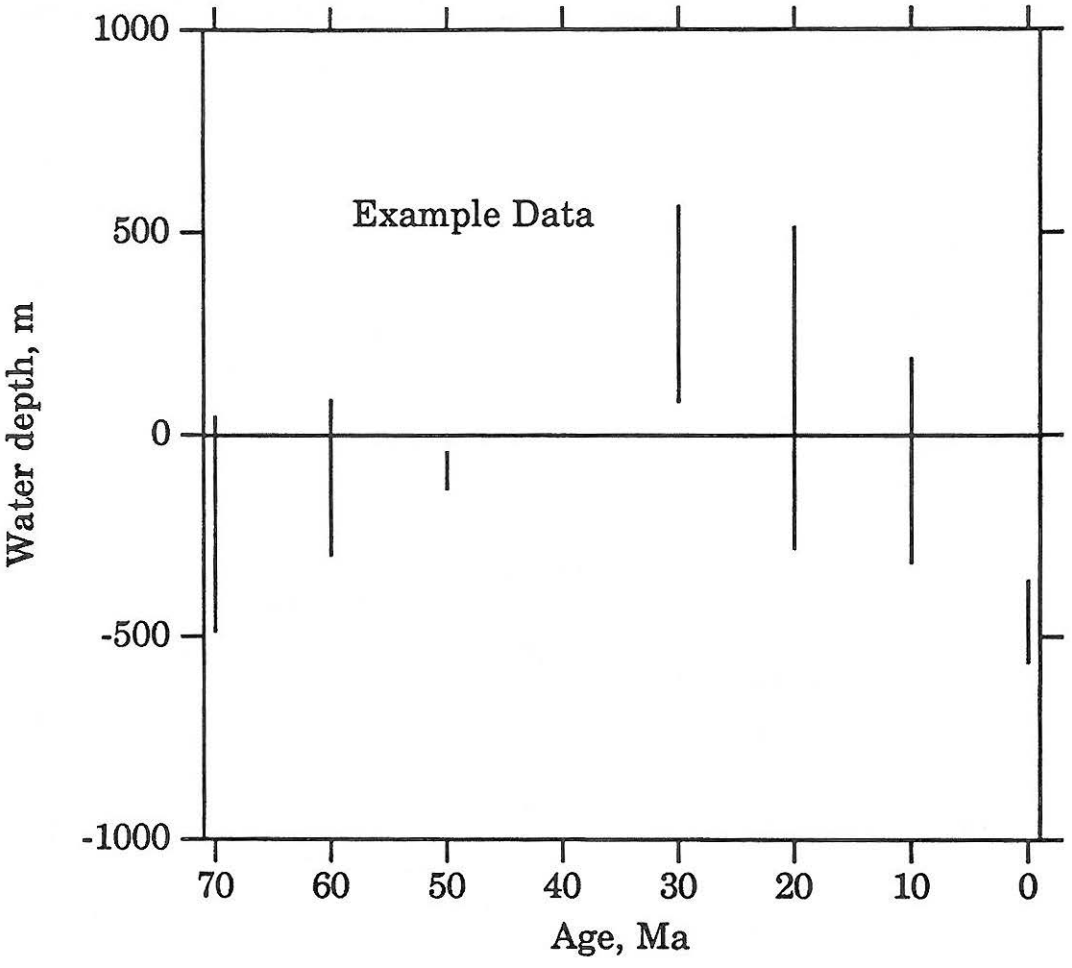

Figure 4.8 Minimum and maximum estimates of water depth variation obtained from Figure 4.7. Water depth variation is based on misfit between tectonic subsidence data and the theoretical subsidence history.

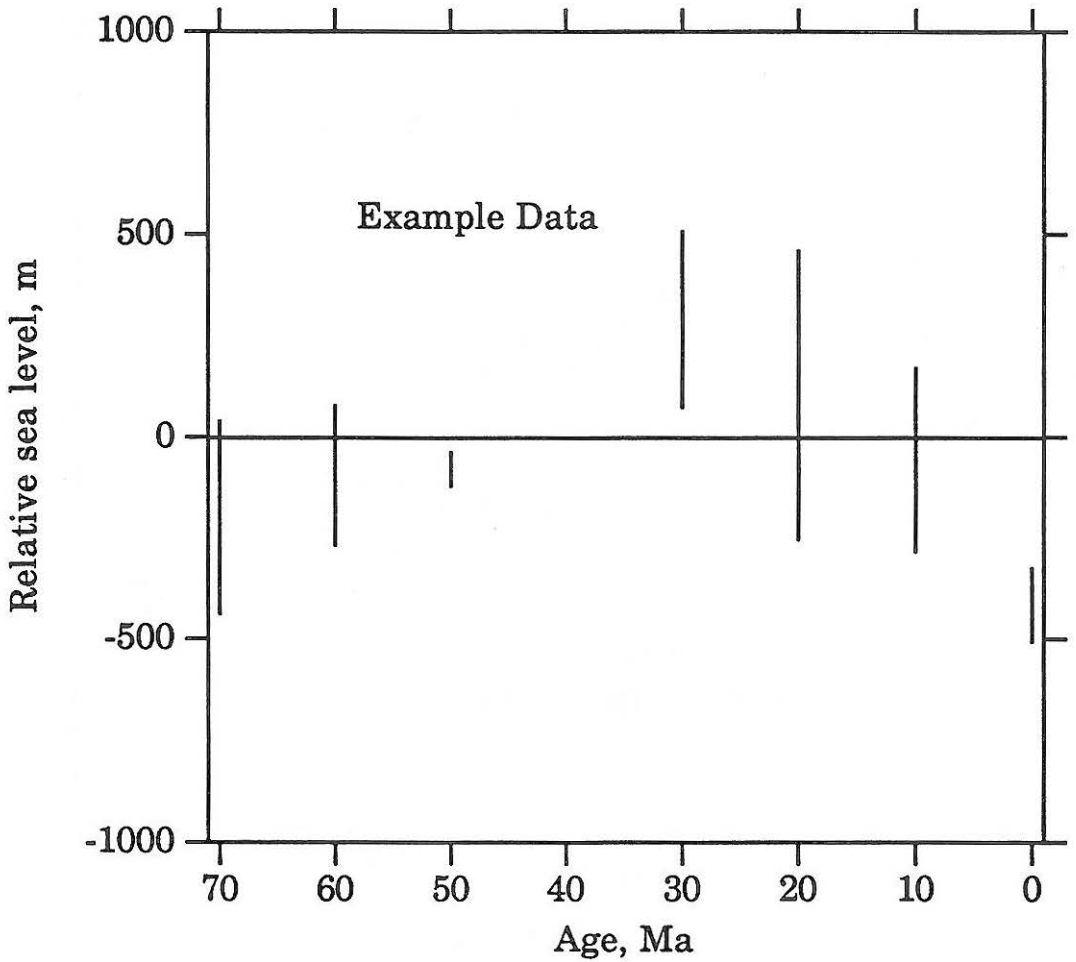

Figure 4.9 Relative sea-level history based on misfit between tectonic subsidence data and best-fitting thermal subsidence history. Relative water depth variation (Fig. 4.8) is corrected for isostatic subsidence due to water loading.

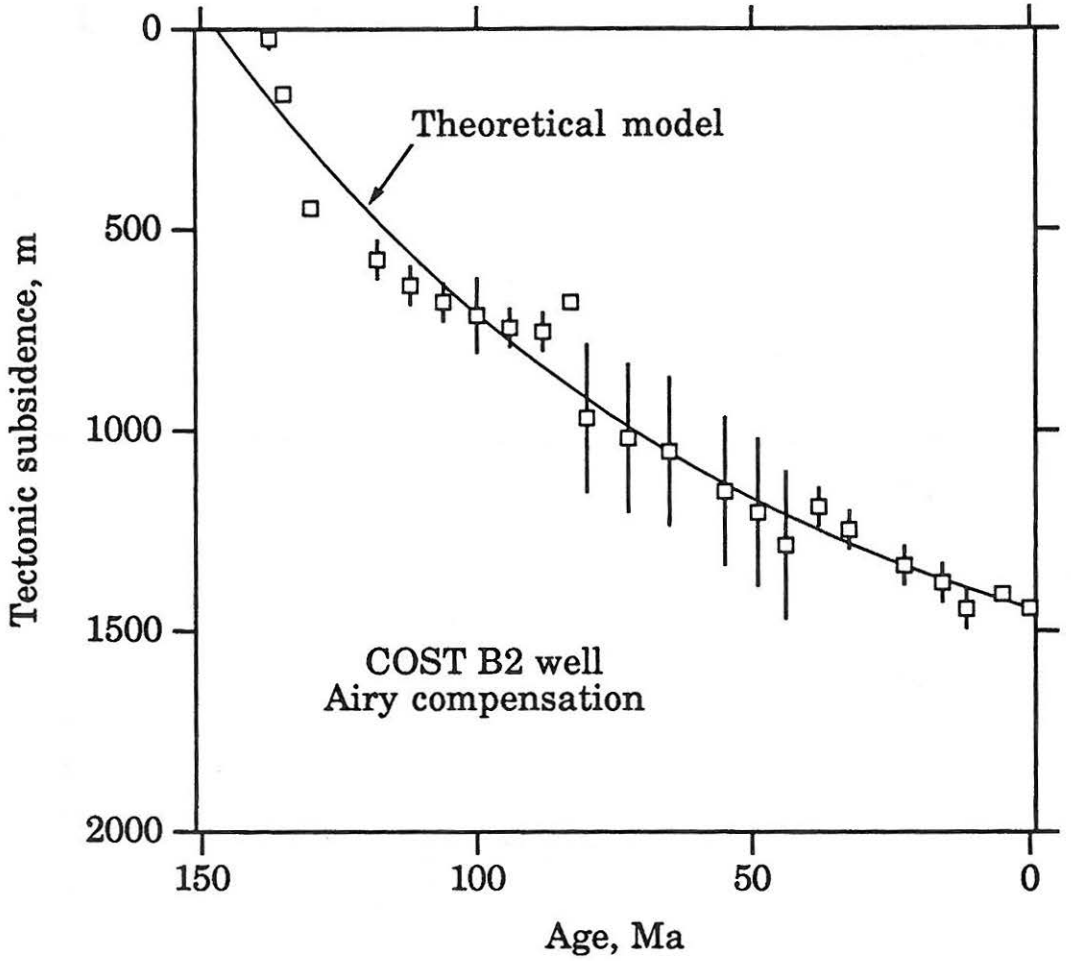

Figure 4.10 Plot showing tectonic subsidence near COST B2 well and best-fitting thermal subsidence model. Backstripping was performed by Steckler and Watts (1978).

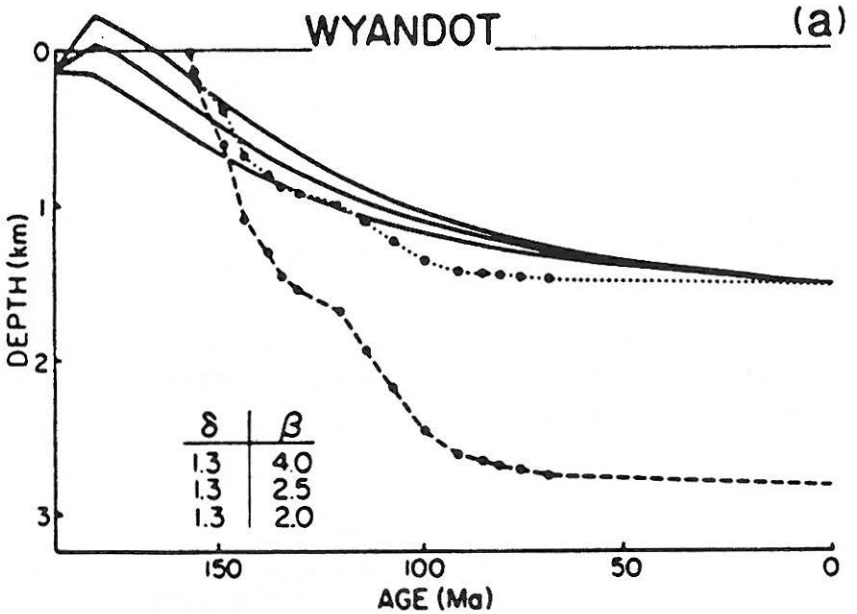

Figure 4.11 Subsidence data from the Nova Scotia shelf (from Royden and Keen, 1980). Attempts to explain tectonic subsidence curve using simple stretching model were unsuccessful due to negligible amount of initial subsidence. Theoretical subsidence curves are based on a nonuniform stretching model (see Fig. 4.12). Mantle lithosphere appears to stretched more than crust.

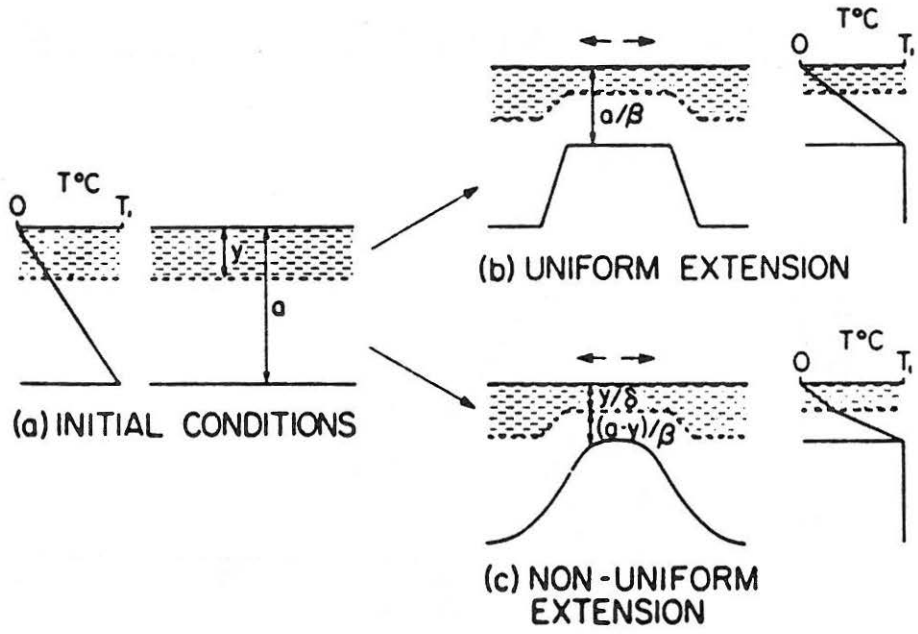

Figure 4.12 Simplified diagram of nonuniform extension model of Royden and Keen (1980). Stretching factors for crust and mantle lithosphere are δ and β, respectively.

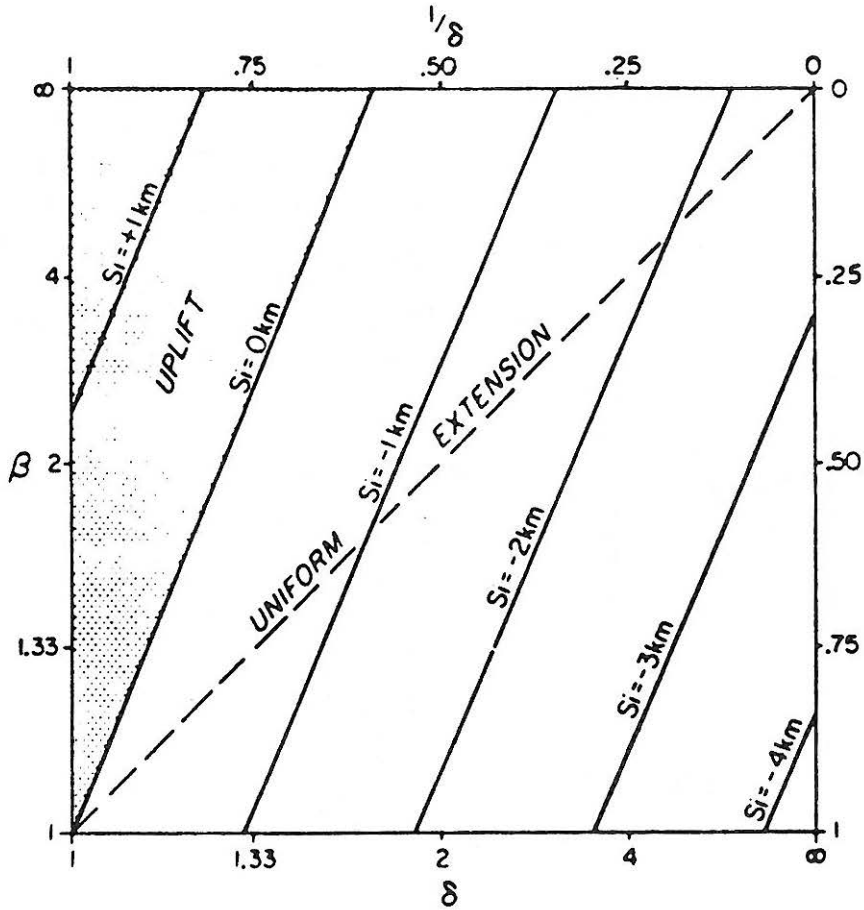

Figure 4.13 Initial subsidence predicted by nonuniform extension model of Royden and Keen (1980). Crust and lithosphere thicknesses are 35 and 125 km respectively.

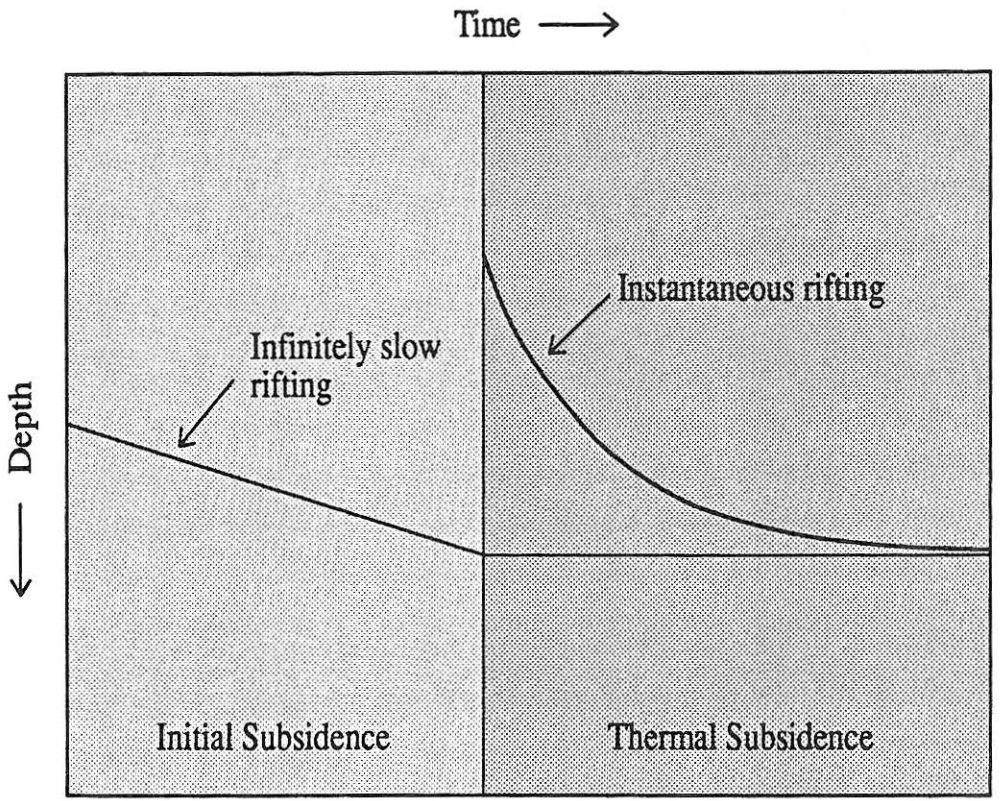

Figure 4.14 Effect of finite rates of rifting on thermal subsidence. If rifting is very slow, the mantle lithosphere will remain cool and little or no thermal subsidence will occur after rifting has ceased.

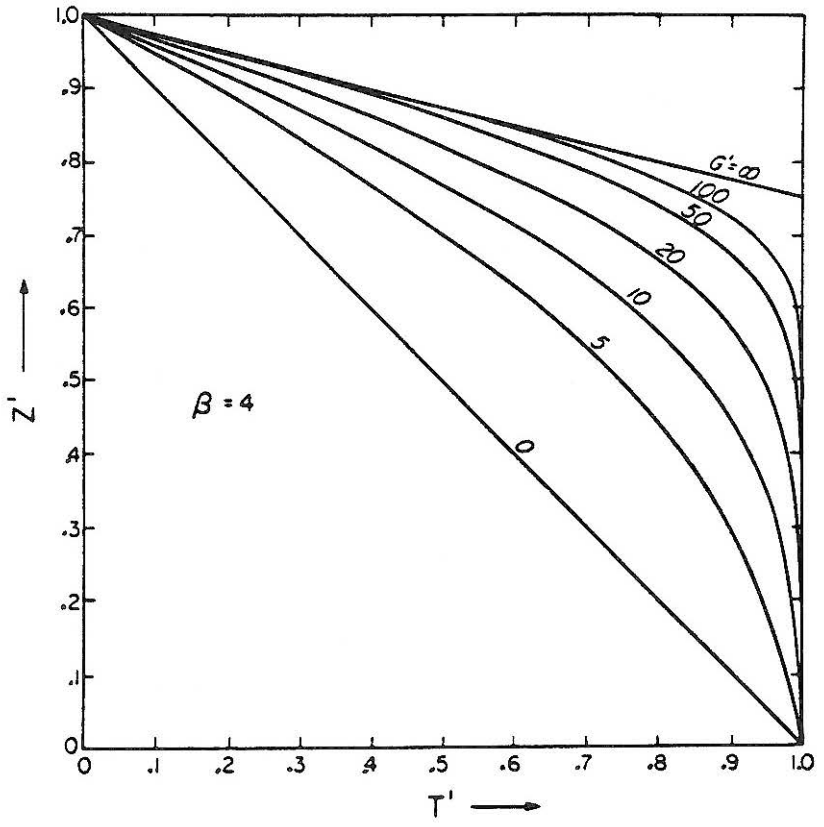

Figure 4.15 Temperature distribution in lithosphere after stretching by a factor of 4 at a constant strain rate (nondimensionalized) G' (from Jarvis and McKenzie, 1980).

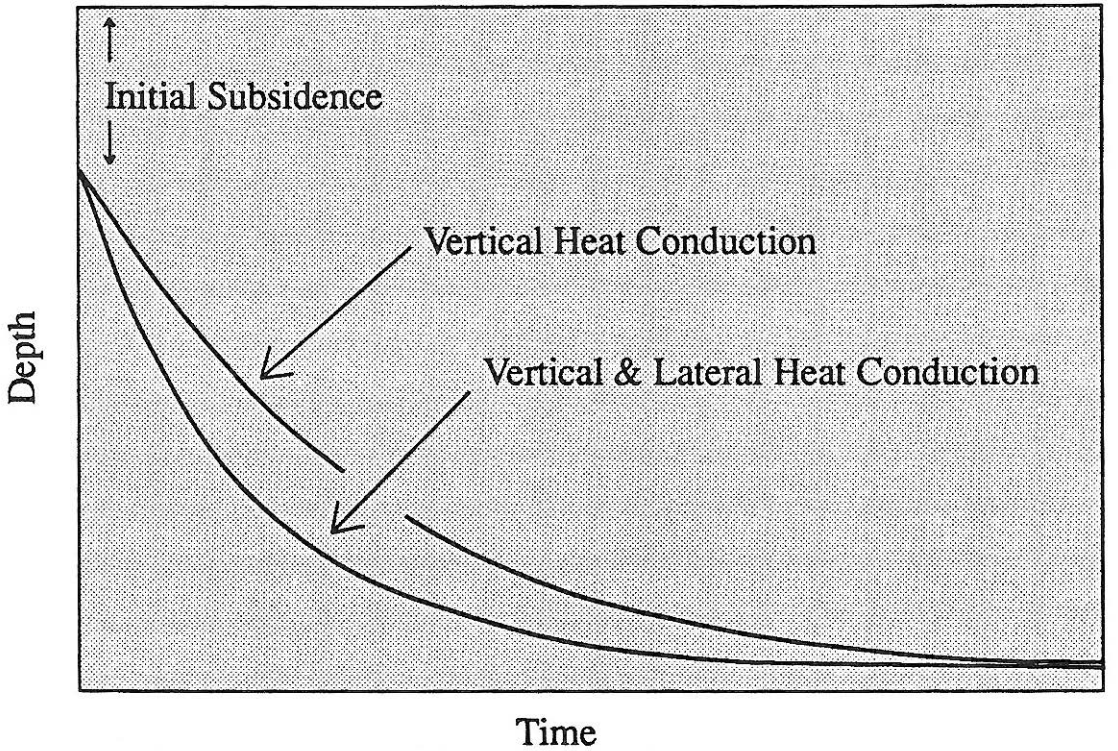

Figure 4.16 Schematic diagram showing the effect of lateral heat conduction on subsidence history near the edge of a rift basin. Lateral heat conduction allows the rift to subside faster than Mckenzie's (1978) simple stretching model predicts.

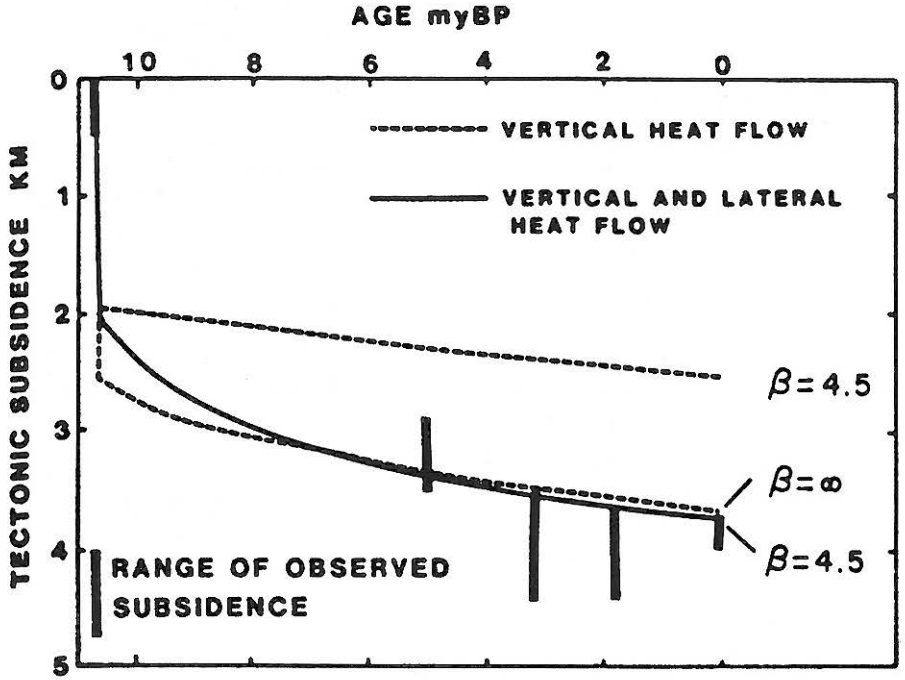

Figure 4.17 Thermal subsidence model for the Los Angeles Basin (from Sawyer et al., 1987) that accounts for both lateral and vertical heat conduction. The model is intended to explain the rapid subsidence observed in the Los Angeles Basin.